Micro-simulation of single-lane traffic to identify critical loading conditions for long-span bridges

OBrien, E.J., Lipari, A. and Caprani, C.C.

1. Introduction

It has been long acknowledged that long-span road bridges are governed by congested traffic rather than free-flowing conditions [1]. In free-flowing traffic, vehicles have large gaps between them, while congestion implies long queues of closely-spaced vehicles. In congested conditions, vehicle-bridge dynamic interaction is not significant, since critical events occur at slow speeds [2, 3]. The bridge length threshold between the two cases depends on many factors but it typically lies between 30 and 50 m [4-6].

Traffic loading for long-span bridges is not taken into account in most codes of practice. The use of short-span bridge load models for the design of longer spans is rather conservative, as the average intensity of loading tends to reduce with increasing span [2, 7, 8]. Excessive conservatism for existing bridges is an even greater problem as it may lead to expensive and unnecessary interventions. In fact, small differences in the traffic loading requirements may imply significant differences in the maintenance operation costs [9].

Real-world observations show that congestion can take different forms, as detailed in Section 2.2. However, most previous studies on bridge traffic loading consider only queues of vehicles at minimum bumper-to-bumper distances [1, 2, 7, 8, 10-14]. Micro-simulation models the behaviour of individual vehicles and allows the generation of observed congestion patterns, thus providing a valuable tool to study the effects of different congestion patterns and traffic compositions on long-span bridge loading. Comprehensive traffic modelling allows a realistic simulation of the traffic scenarios expected to occur on the bridge, and therefore more accurate safety evaluation and more efficient maintenance planning.

1.1 Data collection

Traffic weight data is based on either truck surveys, or, more recently, weigh-in-motion (WIM) measurements. However, it must be noted that many WIM devices deployed on highways can accurately weigh vehicles only at higher speeds and do not work well or at all in stop-and-go traffic. Furthermore, traffic data (such as vehicle counts or speeds) is mostly collected by means of induction loops (sometimes combined with WIM devices), which may not be reliable at very low speeds [15]. As a consequence, data is largely collected during free-flowing traffic conditions, which also occur more frequently than congestion, whereas data about slow-moving – and therefore closely-spaced vehicles – is lacking.

Free-flowing traffic measurements are suitable for the analysis of traffic loading on short-span bridges, whose critical loading is made up of one or two big vehicles (see for instance Buckland et al. [2]). In such cases, the inter-vehicle gaps (or headways) can be taken directly from the WIM

database, or from a calibrated headway model [16]. However, in long-span bridges, congestion governs and the gaps in such condition are mostly unknown, due to the above-mentioned lack of data at low speeds.

Not only is data collection problematic during congestion, but also the analysis of traffic data can pose some issues [17, 18]. As traffic data is generally collected only at point locations, vehicle positions can only be estimated from such point measurements, typically under an assumption of constant speed. However, during congestion, speeds may vary significantly. Therefore the estimation of the maximum number of vehicles present on a stretch of road from point measurements may result in a significant loss of accuracy [19], and bridge loading is obviously affected by the number of vehicles actually present on the bridge. On the other hand, the use of spatial detectors (such as cameras) over a stretch of road allows the collection of the vehicle positions during congestion, without resorting to estimation. Although cameras are the best solution from a theoretical point of view, they have not often been used for several practical reasons, such as sensitivity to illumination changes, communication requirements for transmitting the large amount of data collected, or computational demands of post-processing [15]. They have however been deployed for research purposes [20-24] and are becoming more popular.

In bridge loading studies, only Buckland et al. [2] and Nowak et al. [8] state that they have used video recordings. Ricketts and Page [3] use videos at various UK sites for manual vehicle classification during congestion. OBrien et al. [25] manually analyse videos for a micro-simulation model calibration. Zaurin and Catbas [26] propose a procedure for automatically tracking vehicles in the context of bridge health monitoring.

1.2 Codes of practice and previous research on long-span bridge traffic loading

Research on traffic loading for bridges is often related to studies for developing codes and standards. Existing load models for long-span bridges account for the variability of truck weights, but often assume a mix of cars and heavy vehicles at minimum bumper-to-bumper distances [1, 2, 7, 8, 10-14], which are typically assumed due to the lack of such data, as discussed in the previous section.

The “normal” load model in Eurocode 1 [27] is based on traffic data collected at Auxerre (France), considering 100% trucks in the slow lane for jam situations [28], and later confirmed with a more extensive database [29]. Its application is valid for the design of bridges up to 200 m. Other national codes, for example the former British and the Italian ones, suggest loading values for longer spans [30, 31]. A recently-withdrawn standard by the Highways Agency [32] prescribed two levels of *Assessment Live Loading* for the assessment of spans longer than 50 m in the United Kingdom; however, current British standards limit the application of the *Assessment Live Loading* to 50 m [33].

The current load model by the American Association of State Highway and Transportation Officials (AASHTO) [34] may be considered to apply to “ordinary bridges” with spans up to 152 m [35, 36], although, in the calibration of its current traffic load model, the maximum span considered is 60 m [37]. The AASHTO load model is lighter than that prescribed in the Eurocode [8]. Lutomirska [38] concludes that the AASHTO load model can be extended to most spans up to 1500 m. Previously, the American Society of Civil Engineers (ASCE) [39] recommended a load model for the design of spans

up to 1951 m, based on the work of Buckland et al. [2]. For assessment, the AASHTO [40] prescribes a "legal" vehicle for the rating of existing bridges longer than 60 m.

Besides codes and standards, Ivy et al. [1] record 5629 heavy vehicles on a long-span bridge in San Francisco; the trucks were all placed at an average distance recorded in the field. Harman et al. [10] develop a procedure for predicting live-load effects using traffic surveys. The Flint and Neill Partnership [7] uses truck surveys and free flow data to build up queues of heavy vehicles and cars; the results are then extrapolated to find the design bridge loading. Vrouwenvelder and Waarts [11] develop a load model based on data from the Netherlands, differentiating between free, congested, and full-stop traffic. Ditlevsen and Madsen [12] develop a theoretical framework for building up queues based on a cell discretisation of the bridge. Bailey and Bez [13] develop a methodology to derive probability distributions of extreme traffic actions based on site-specific data; they differentiate between traffic conditions of free, congested, and at-rest, and assign a probability distribution to gaps. Nowak et al. [8] use WIM data and videos of congested traffic to develop a design load model made up of an average heavy-vehicle queue on the slow lane.

Table 1 lists the assumed congested inter-vehicle gaps in selected models, as well as their stated span length application. Note that, in spite of the fact that such gaps are deemed representative of traffic at a standstill, the vehicles are generally moved along the bridge: the first vehicle is removed, the queue is then moved forward, and a vehicle is added at the other end of the bridge. All of these methods exclude the observed variability of congested patterns, with the exception of Vrouwenvelder and Waarts [11] and Bailey and Bez [13]; however, the underlying traffic models were quite basic, with all the vehicles moved at the same constant speed. Furthermore, the frequencies of occurrence of congestion are assumed or based on little data, and are generally rather conservative.

Table 1
Congested gap and span length application for selected existing load models.

Model	Congested gap (m)	Span length application (m)
Ivy et al. [1]	2.4	>120
ASCE (Buckland et al. [2])	1.5	15–1951
Flint and Neill Partnership [7]	0.9–1.8	75–1600
Vrouwenvelder and Waarts [11]	1–10	2–200
Eurocode 1 (Prat [14])	5[a]	5–200
Nowak et al. [8]	4.5	180–1500

[a] Between subsequent axles.

Recently, traffic micro-simulation has been used to achieve a more accurate traffic modelling, with special regard to the variability of inter-vehicle gaps, with the notable advantage that the widely-available free-flowing traffic measurements can be used as initial conditions for simulating congested traffic scenarios. OBrien et al. [25] study a long-span bridge in the Netherlands and calibrate a commercial micro-simulation tool using WIM data, videos and strain gauge measurements. Chen and Wu [41] use the cellular automaton approach (initially proposed by Nagel and Schreckenberg [42]), in which the bridge is divided into 7.5 m cells. However, the cellular structure does not allow for the variability of vehicle lengths and gaps between vehicles, and this is

quite important in bridge loading. Caprani [43] uses micro-simulation to calibrate a simple congested load model for short- to medium-length bridges, whereas Enright et al. [44] use micro-simulation to compare European and American load models for long-span bridges.

2. Micro-simulation

Micro-simulation is widely used in traffic engineering with many models having been developed over the last few decades [45-47]. Micro-simulation takes account of the interaction between vehicles, thus introducing driver behaviour into the model. It is possible to characterise each vehicle with its own vehicle properties and driver behaviour, but this is often not necessary, as will be discussed later.

Free-flowing traffic measurement can be used to generate initial traffic condition but congested data may be still required for calibration and validation [48, 49]. Broadly speaking, no micro-simulation model has been found to give a totally reliable reproduction of observed traffic; therefore the choice of the model mainly relies upon the traffic features of interest, e.g. during free-flowing traffic or congestion, in urban or extra-urban environment, etc. For bridge loading applications, it is essential that the micro-simulation model be able to reproduce the variety of congested patterns, mostly neglected in previous bridge loading research.

Micro-simulation models divide into car-following (single-lane) and lane-changing (multi-lane) models. In this paper, a car-following model is used which has been found to replicate many observed congestion patterns on several motorways [50]. The micro-simulation approach has been programmed in-house and the program is known as SIMBA (SIMulation for Bridge Assessment). The focus here is to identify congested states which may be critical for long-span bridge loading.

Single-lane micro-simulations are carried out considering a high inflow rate, representative of peak hour traffic. Different truck percentages are randomly injected amongst the car flow. Several types of congestion are generated over a stretch of road, encompassing two long-span bridges (200 and 1000 m long).

Lane-changing models are less established than car-following models, mainly due to practical difficulties in tracking the several vehicles involved in a single lane-changing manoeuvre. However, lane change activity is known to be low during congestion [51], as there are few gaps available to move into an adjacent lane, thus making the present single-lane approach relevant to multi-lane roadways as well. Indeed, the consideration of a high truck percentages can represent the slow lane of a multi-lane roadway, where the vast majority of trucks are often concentrated [52].

2.1 The Intelligent Driver Model

The *Intelligent Driver Model* (IDM) is a car-following model that has successfully replicated several congested traffic patterns observed on some German *multi-lane* motorways. This was achieved by modelling a *single-lane* traffic stream made up of identical vehicles with constant parameters [50], thus significantly easing the calibration process and the computational burden while retaining the desired capability of replicating congested traffic patterns.

The correspondence between simulated and observed traffic patterns is mainly *qualitative*, thus making a quantification of the accuracy problematic, although there are recent attempts to quantify it [53]. However, the model accuracy is easier to quantify and verify when comparing single vehicle trajectory data, thereby allowing a comparison with other car-following models [54-56]. In this case, the IDM returns results comparable to more complex models [57, 58], with indicative relative errors in the order of 15%.

The motion of each vehicle over time is simulated through an acceleration function:

$$\frac{dv(t)}{dt} = a \cdot \left[1 - \left(\frac{v(t)}{v_0} \right)^4 - \left(\frac{s^*(t)}{s(t)} \right)^2 \right] \tag{1}$$

where a is the maximum acceleration, v_0 the desired speed, $v(t)$ the current speed, $s(t)$ the current gap to the front vehicle, and $s^*(t)$ the minimum desired gap, given by:

$$s^*(t) = s_0 + Tv(t) + \frac{v(t)\Delta v(t)}{2\sqrt{ab}} \tag{2}$$

in which, s_0 is the minimum jam (bumper-to-bumper) distance, T the safe time headway, $\Delta v(t)$ the speed difference between the current vehicle and the vehicle in front, and b the comfortable deceleration. There are only five parameters in this model to capture driver behaviour, which are relatively easy to quantify, for instance analysing loop detector data [50]. For modelling purposes, the length of the vehicles l must also be specified. Equations (1) and (2) are solved with discretisation into 0.25 s steps.

In the following the parameters are briefly outlined, as well as their main effects on the traffic stream. For a comprehensive discussion, including calibration of the parameters, the reader is referred to Treiber et al. [50] or Treiber and Kesting [59].

The desired speed v_0 is the speed a vehicle reaches on a '"free road'", i.e. with no other vehicles in front ($s = \infty$). The maximum acceleration a gives the acceleration from a standstill on a free road. The acceleration on a free road decreases with increasing speed v (Equation 1), reaching zero at $v = v_0$. The comfortable deceleration b adjusts the braking behaviour when approaching a slower or stopped vehicle; in particular, b is the maximum deceleration that a driver will accept in non-emergency situations.

An explicit definition of the safe time headway parameter T is not straightforward: however, it can be more easily understood in the case when all the vehicles drive at the same speed ($\Delta v = 0$ in Equation 2) and traffic is not free-flowing ($v << v_0$ in Equation 1). In such a case, the (safe) distance s a vehicle keeps when following its leader is mainly determined by a fixed term, that is the parameter *minimum jam distance* s_0, and a speed-dependent term, regulated by the parameter *safe time headway* T, i.e. $s \approx s^* = s_0 + v\,T$. Smaller T or s_0 implies closer vehicles and then greater load. Most importantly for bridge loading applications, the sum $l + s_0$ determines the maximum possible number of vehicles present on a bridge, i.e. when they are at a standstill ($v = 0$).

The traffic flow stability is the response of the traffic flow to a perturbation, e.g. a braking vehicle. If the traffic flow is unstable, then a perturbation will propagate into a *stop-and-go wave*, thus breaking down the traffic flow and potentially leading to critical bridge loading events. The stability behaviour is mainly determined by the model parameters *a*, *b*, and *T*. Traffic is more unstable for smaller *a* and *T*, and larger *b*. Here it is most important to note that the stability of multi-class traffic (e.g. made of cars and trucks) is essentially equivalent to single-class traffic with averaged parameters [60]. Hence, the adoption of different parameter sets for cars and trucks is not strictly necessary for reproducing the congested patterns, nor the adoption of variable parameters among vehicles of the same class.

2.2 Congested Traffic States

Treiber et al. [50] show that congestion can be effectively generated by either locally decreasing the desired speed v_0 or increasing the safe time headway *T*. Such a way of generating congestion is named *flow-conserving inhomogeneity* [50] and disrupts the traffic in a similar way to on-ramp bottlenecks or lane closures. In this paper, inhomogeneity is generated by increasing the safe time headway *T* downstream, say *T'*, which Treiber et al. [50] state to be more effective than decreasing v_0.

The bottleneck strength ΔQ can be defined as the difference between the outflow Q_{out} with the original parameter set and the reduced outflow Q'_{out} with the modified safe time headway *T'*:

$$\Delta Q(T') = Q_{out}(T) - Q'_{out}(T') \tag{3}$$

The outflow here is the *dynamic capacity*, that is, the outflow from a congested state. It is well established that, after traffic flow breaks down, the maximum outflow drops from the static capacity Q_{max} to a value related to the discharge rate of the queue [61-63], which is the dynamic capacity Q_{out}. The bottleneck strength can be also computed as an equivalent on-ramp inflow [64]. For practical applications, the velocity at the detector nearest to the bottleneck can also be used as a proxy for the bottleneck strength [53].

A smaller safe time headway *T* implies closer vehicles, thus increasing the dynamic capacity Q_{out}. This implies that greater values of reduced capacity Q'_{out} (i.e. greater inhomogeneities, or traffic disruptions) are needed to generate the same bottleneck strength ΔQ (Equation 3). This, in turn, decreases the probability of congestion events and consequently the probability of critical bridge loading scenarios. This "stabilising" effect due to a smaller *T* contrasts with the increase in loading mentioned in Section 2.1.

Depending on the inflow Q_{in} and the bottleneck strength ΔQ, and for a given traffic history, the downstream traffic can take up any of the traffic states explained in Table 2 [50, 64]. Such states can be typically identified through analysis of speed data from loop detectors. A combination of these congested states may also occur. In general, increasing inflow and/or bottleneck strength has the effect of moving down the table to a higher intensity of congestion. Congested states that occupy a significantly long stretch of road (the so-called *extended* states), namely SGW, OCT and HCT, are of significance for long-span bridge loading applications and are dealt with below.

Table 2
Congested traffic states.

Acronym	Explanation of traffic state
FT	Free Traffic
MLC	Moving Localized Cluster
PLC	Pinned Localized Cluster
SGW	Stop and Go Waves
OCT	Oscillatory Congested Traffic
HCT	Homogeneous Congested Traffic

A trajectory plot is a graph showing the location of many vehicles through time. The slope of each vehicle trajectory curve is proportional to its speed. An example of typical trajectory data for traffic made up of identical vehicles is given for two bottleneck strengths in Figure 1 (for the parameters, see the car set in Table 3). Figure 1(a) shows a typical SGW state. Each vehicle goes through cycles of slower and faster travel (low slope and steep slope). The bands of congestion (waves) propagate backwards at about 10 km/h, which is in the lower range of typical observed wave propagation speeds, while there is no typical wavelength or period [64, 65]. In between the waves, drivers recover speed up to 60 km/h before meeting another wave. Figure 1(b) shows an OCT state in which waves exist but are less pronounced. The waves keep their characteristic propagation speed, but they are closer and the speed amplitude is less, as vehicles rarely exceed 40 km/h in between the waves. The downstream speed amplitude is even smaller, getting close to a HCT state, which shows no oscillations at all.

2.3 Multi-class simulations

Treiber et al. [50] successfully use only identical vehicles to simulate multi-class traffic. However, in this research trucks need to be introduced, as they are the most significant source of bridge load. It is well known that truck presence reduces the capacity of a road [63]. Therefore, traffic streams with different truck percentages have different dynamic capacities Q_{out}, which affect the bottleneck strength ΔQ through Equation (3), and subsequently the expected congested state. In order to make a meaningful comparison between congested states with different truck percentages, it is important that the effects on traffic be equivalent, that is, pairs of $Q_{in}/\Delta Q$ that return the same congestion must be found. The Highway Capacity Manual [63] suggests *heavy-vehicle adjustment factors* f_{hv} in order to relate the (static) capacity of mixed traffic to the capacity of a base flow made up of passenger cars only. A similar equivalence is set out here in terms of the dynamic capacity Q_{out}, i.e. heavy-vehicle adjustment factors are computed in order to relate the dynamic capacity of mixed traffic to that of a flow with no trucks [19].

Truck proportions of 20% and 50% are randomly injected between cars. The lesser percentage is adopted as a common truck percentage on a busy commercial route, while the greater percentage accounts for slow lanes of multi-lane carriageways, which typically have a greater truck percentage in the slow lane. Note also that such a high percentage is possible when the flow is low, typically in the early morning or at night [3, 7, 66, 67].

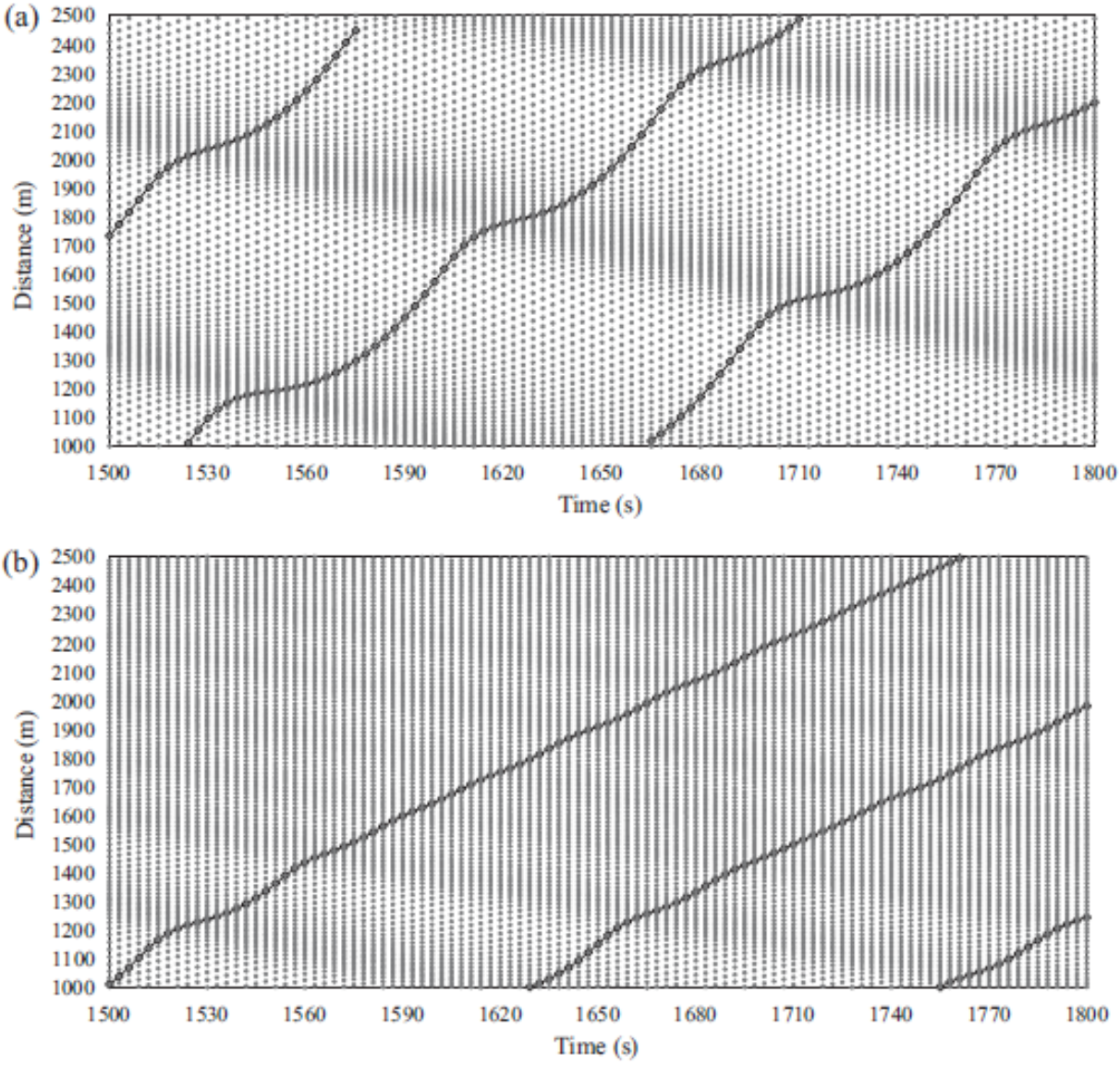

Fig. 1. Example of trajectory data for (a) SGW and (b) OCT; trajectories of vehicle Nos. 650, 700 and 750 are highlighted.

Table 3
Model parameters.

Parameter	Car	Truck
Desired speed, v_0	120 km/h	80 km/h
Safe time headway, T	1.6 s	1.6 s
Maximum acceleration, a	0.73 m/s^2	0.73 m/s^2
Comfortable deceleration, b	1.67 m/s^2	1.67 m/s^2
Minimum jam distance, s_0	2 m	2 m
Vehicle length, l	4 m	12 m
Gross vehicle weight, GVW	20 kN	432 kN[a]

[a] Normally distributed with CoV = 0.1.

Table 4 gives the dynamic capacity Q_{out} for the mixed traffic conditions and the relevant heavy-vehicle adjustment factors f_{hv} for Q_{out}, as well as the static capacity Q_{max} (which can be attained only in uncongested traffic). The reference condition of 0% trucks and the condition of 100% trucks are included for comparison. For the parameter set chosen (Table 3), Q_{out} and Q_{max} are quite close, whereas in real traffic the difference may be higher [61, 62]. However, the IDM has been calibrated to reproduce observed congested states [50], which are critical for long-span bridge loading.

Table 4
Capacity of multi-class traffic.

Truck percentage (%)	Q_{out} (veh/h)	f_{hv}	Q_{max} (veh/h)	Q_{out}/Q_{max}
0	1686	1.00	1790	0.94
20	1590	0.94	1630	0.98
50	1462	0.87	1489	0.98
100	1291	0.77	1311	0.98

3. Model and Simulation Parameters

3.1 Traffic stream

In order to minimize the number of variables while retaining the essential features of the problem, the vehicle stream is taken as being made up of two classes: cars and trucks. Each vehicle of the same class is given the same set of parameters, shown in Table 3. Due to the mentioned lack of congested data, the parameter set is based on that calibrated and used by Treiber et al. [50], who use identical vehicles, as discussed above. However, trucks need to be introduced here and are assigned greater length and weight, and a smaller desired speed v_0 [48, 68]. Trucks are also more inert (i.e., smaller a and b): however, these parameters are difficult to quantify, unlike the desired speed v_0, and therefore the same calibrated parameters suggested in Treiber et al. [50] are adopted.

To reduce the variables of the problem so that the influence of traffic congestion is isolated, a standard truck configuration is adopted with mean gross vehicle weight (GVW) taken as the minimum European legal limit of 44 t [69] and normally distributed with a Coefficient of Variation (CoV) of 0.1. The distribution of weight between axles (Figure 2) is representative of the Auxerre traffic on which the Eurocode load model is based [70]. Front and back overhangs of 0.9 m are assumed. The assumed truck distribution is rather heavy and is not meant to represent actual traffic. These simplifications are deliberate – they seek to keep the underlying assumptions about the traffic stream as simple as possible in order to clearly identify the effect of different congestion patterns on loading.

3.2 Road geometry and bottleneck strength

A single-lane 5000 m long road is used in this work. The IDM parameter safe time headway is T from 0 to 2700 m (see Table 3), then increases gradually to the value T' at 3300 m in order to generate congestion (see Section 2.2). A range of values for T' (and consequently bottleneck strengths, ΔQ) are considered: 1.9, 2.2, 2.8, 4.0, and 6.4 s. The inflows Q_{in} are set equal to the dynamic capacity, Q_{out}, corresponding to the relevant truck percentage (Table 4).

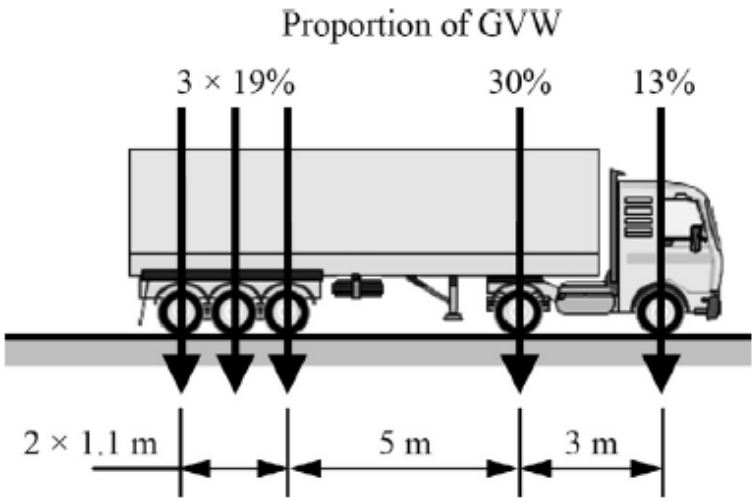

Fig. 2. Assumed truck configuration and axle weight proportions of GVW.

The *equivalent bottleneck strength*, ΔQ_{eq}, that is the bottleneck strength corresponding to an equivalent passenger car-only traffic stream, is given by:

$$\Delta Q_{eq}(T') = \frac{\Delta Q(T')}{f_{hv}} \tag{4}$$

Figure 3 shows the relationship between the applied inhomogeneity, $\Delta T = T - T'$, and the resulting equivalent bottleneck strength. It can be seen that same inhomogeneities return similar equivalent bottleneck strengths, ΔQ_{eq}, regardless of the percentage of trucks, and therefore similar congestion patterns are expected.

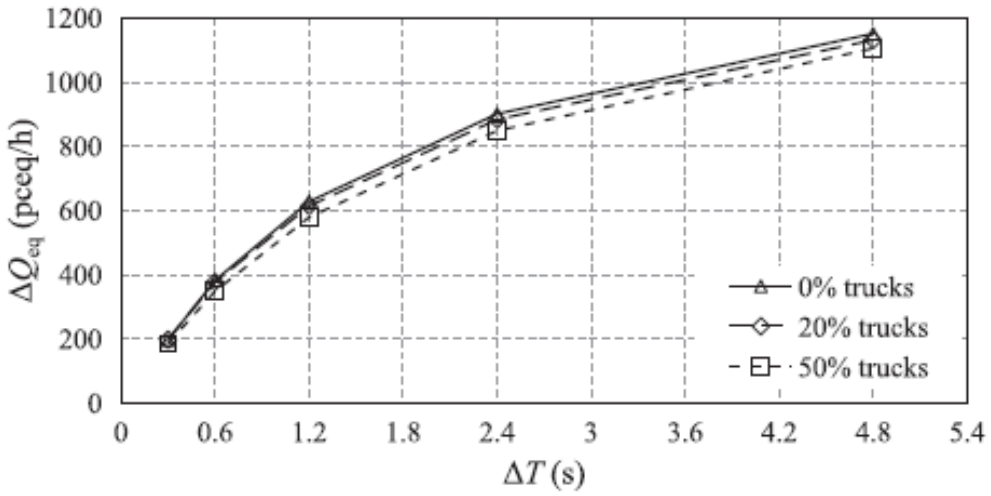

Fig. 3. Equivalent bottleneck strength.

For comparison with the common traffic loading assumption, the full-stop condition (FS) is also simulated. This corresponds to $\Delta T = \infty$ or $Q'_{out} = 0$ veh/h. Then the equivalent bottleneck strength ΔQ_{eq} is 1686 passenger-car equivalents per hour (pceq/h), according to Equation (3).

Finally, it is assumed that the road is affected by one hour of congestion each working day of a 250-day year. Two years of congested traffic are simulated for each bottleneck strength and truck percentage, for a total of over 9.1 million vehicles generated and 6000 hours of congestion analysed.

4. Traffic results

4.1 Spatio-temporal congestion plots

Spatio-temporal plots are useful for visualizing congested patterns. It is convenient to draw a comparison in terms of local mean speed over the congested space-time domain, since flow and density vary significantly depending on the truck percentage. In traffic theory, there are two variables to describe the mean speed: the *time* and the *space* mean speed, depending on whether speed is averaged at a certain point over a time interval, or at an instant of time over a stretch of road. The latter is the more formally correct and is used here. The *space mean speed* can be reasonably approximated as the harmonic mean of the individual speeds collected at one point (this definition is exact only when there are no accelerations or decelerations). For further details and discussion, the reader is referred to Wardrop [71] or Hall [72].

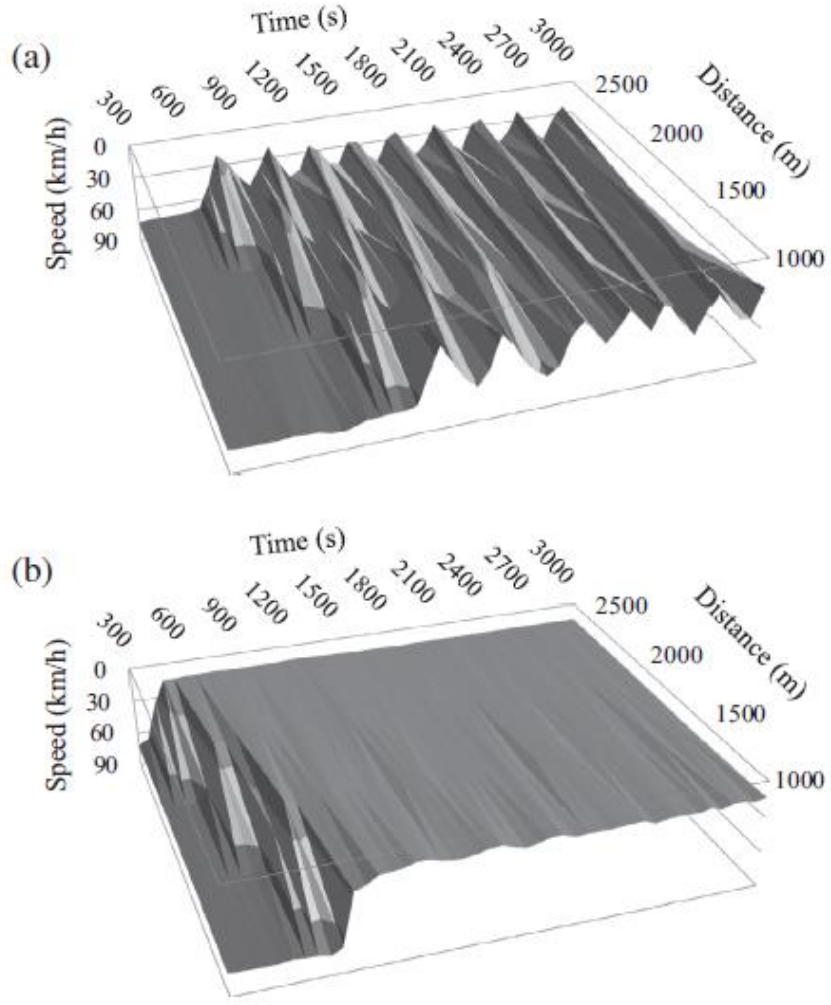

Fig. 4. Spatio-temporal speed plots of (a) SGW and (b) HCT/OCT with 20% trucks.

The space mean speed is collected at four virtual point detectors placed between 1000 and 2500 m and is aggregated in 60 s intervals. The speed axis is depicted upside down so that peaks represent congestion. Figure 4(a) shows an SGW state, where the waves are clearly visible as peaks. Figure 4(b) shows a combined HCT/OCT state, where the upstream small oscillations typical of the OCT state fade away into a HCT state downstream, where there are essentially no oscillations.

4.2 Effects of truck percentage

After determining the heavy-vehicle adjustment factors f_{hv} for the different traffic compositions analysed (Table 4), it is useful to see how the traffic characteristics change in response to the varying truck percentages. Figure 5(a) shows that the traffic is actually quite similar in terms of average space mean speed over the congested area 1000-2500 m. The congested states deriving from the applied bottleneck strengths are also depicted. Note that two HCT states are generated, which differ in the average speed and are labelled HCT(1) and HCT(2), representing about 9 km/h and 5 km/h respectively. The latter, in particular, represents a very heavy state of congestion, where vehicles are spaced at about 4.5 m.

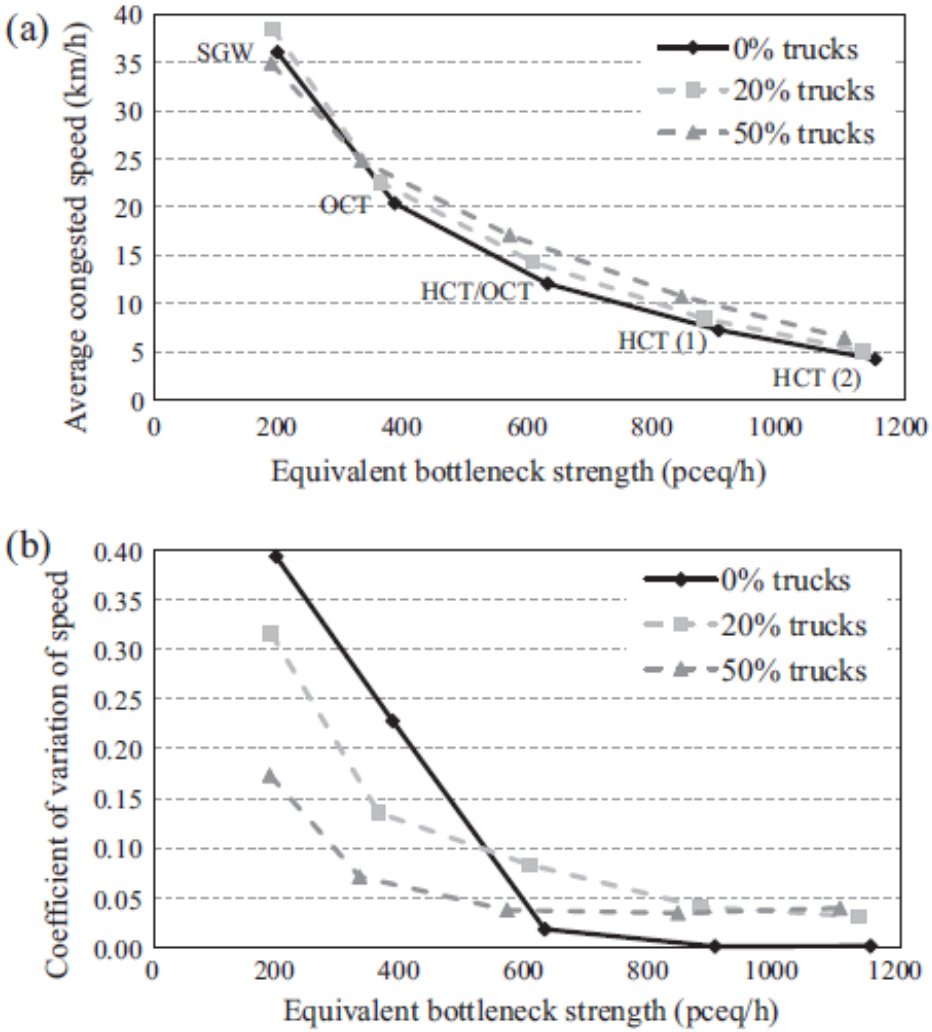

Fig. 5. Distribution of speed in the congested area: (a) average and (b) coefficient of variation.

It is also interesting to consider the traffic oscillation properties, which shows a greater sensitivity to the truck percentage (Figure 5(b)). A greater coefficient of variation of the speed indicates prominent oscillatory behaviour. Indeed the lightest bottleneck strengths show a high coefficient of variation, which reduces as the bottleneck strength increases. The truck presence actually dampens the speed oscillations at the lightest bottlenecks, probably due to their slower desired speed. On the other hand, their different properties introduce a small disturbance in the homogenous congested states which, in the absence of trucks, show no oscillations.

5. Loads on bridges

5.1 Introduction

In this section, the total load on two long spans (200 and 1000 m) is computed. The bridges are placed upstream of the inhomogeneity and centred at 2000 m in the 5000 m length of roadway modelled. The maximum total load for each one-hour congestion event is captured. The total bridge load is computed directly from the actual spatial distribution of vehicles (as the sum of the weights of the vehicles present on the bridge), thus avoiding any inaccuracy due to the estimation of the vehicle positions from point measurements (see Section 1.1).

As traffic micro-simulation is able to reproduce realistic spatial distributions of cars and trucks, it is a suitable tool to investigate stresses on bridges, without resorting to conservative assumptions about heavy vehicle positions. However, while the adopted procedure may be fully used to output stress or stress resultants, such as bending moment [19, 73], this requires the choice of a structural form for the bridges to be analysed. Since such forms may be quite different for long spans, the use of the total load is adopted here to maintain the generality of the study.

Assuming one hour of congestion per day, the hourly/daily maximum values of the total load are extrapolated to determine 5-year characteristic values, in order to limit the effect of the extrapolation procedure on the final result. Doing so assumes that only one type of congestion occurs during the 5-year period. The issue of mixing different congestion types is addressed in Section 6.

As is common in traffic loading studies, a probabilistic approach is used for determining the load, z, which has a given probability of non-exceedance, $F(z)$, also expressed in terms of return period, $T(z)$ [74]. The two variables are linked through the relation:

$$T(z)=\frac{1}{1-F(z)} \tag{5}$$

The *Generalised Extreme Value* (GEV) distribution is fitted to the simulated hourly/daily maximum total loads. The probability F that a load level, z, is not exceeded is [74]:

$$F(z)=\exp\left\{-\left[1+\xi\left(\frac{z-\mu}{\sigma}\right)\right]^{-\frac{1}{\xi}}\right\} \tag{6}$$

in which μ is the location, σ the scale, and ξ the shape parameter. Equation (6) is defined for any value z for which $1+\xi\left(\frac{z-\mu}{\sigma}\right)>0$. When ξ = 0, the GEV distribution reduces to the Gumbel distribution.

Gumbel probability paper is used to illustrate the extrapolation procedure [75]. On this scale, data from a Gumbel distribution appears as a straight line. The *y*-axis ordinate, or *Standard Extremal Variate* (SEV), is given by:

$$SEV(z) = -\log\left[-\log\left(F(z)\right)\right] \tag{7}$$

For the 5-year return period and with 250 working days per year, the target probability of non-exceedance $F(z^*)$ is 0.9992 (Equation 5) and the target SEV is 7.13 (Equation 7).

The GEV parameters are inferred through maximum likelihood estimation (for details, see Coles [74]).

5.2 Results for 200 m bridge

The probability paper plots for the 200m span are shown in Figure 6, as well as the 5-year characteristic hourly/daily maximum values z^*. The hourly maximum values for free-flowing traffic are shown for reference and can be seen on the left-hand side of the plot, to be quite separate from the congested ones. The distribution for the combination of congestions is also plotted and is addressed in Section 6.

It can be seen that the different congestion types are separate from each other and that greater bottleneck strength implies greater load, with the exception of the FS condition. Figure 6(a) gives results for the more common case of 20% trucks. Most trends curve upwards, suggesting compliance with the Weibull distribution ($\xi < 0$). The Weibull distribution indicates data for which there is an upper limit, i.e., there is a limiting level which is not exceeded as the cumulative probability approaches unity. Note that the Weibull distributions also indicate a small sensitivity to the previous assumption on the number of hours of congestion: for instance, if the simulated 500 hours of congestion represented 5 years' traffic (rather than 2), the corresponding 5-year characteristic load would be at the ordinate of the highest simulated point, i.e. at the target SEV of 6.22 (Equation 7), with comparable values of load and, most importantly, no changes in the order of the congestion patterns critical for bridge loading.

The two full HCTs found are the most critical congested states, whereas FS tends to be low because it is the maximum of just one realisation of truck weights. In other words, the slow-moving HCT states give more combinations of vehicles (and subsequently more probability of finding an extreme loading), whereas the FS gives only one, although vehicles are at the minimum bumper-to-bumper distance s_0.

The high truck percentage (Figure 6(b)) has the effect of reducing the variability of truck concentrations, so that the load values of each congestion type are concentrated on a smaller range (as a smaller scale parameter σ shows, Table 5). Several maxima for the full-stop condition are

relatively low (see also Figure 7), but for high return periods the characteristic value exceeds all others.

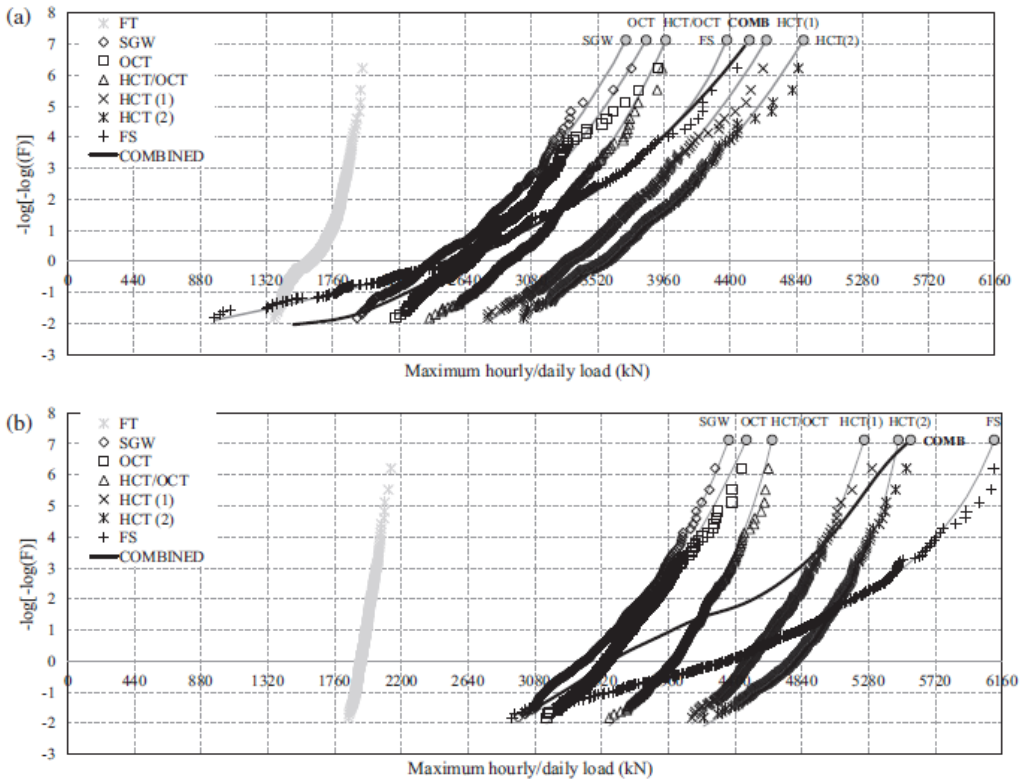

Fig. 6. Probability paper plot of total load on 200 m span with (a) 20% and (b) 50% trucks; each vertical gridline approximately represents the weight of one average truck.

The average hourly/daily maxima are illustrated in Figure 7. The general trend is one of linearly increasing total load with increasing bottleneck strength, with the exception of the average FS condition for the reasons discussed above. The GEV parameters for the maximum likelihood fits are given in Table 5 for all cases, along with the characteristic maximum total loads. FS conditions have a greater scale parameter σ, indicating more scattering across the load range, and smaller shape parameter ξ, indicating higher curvature upwards.

Table 5
Parameters and extrapolated values of the GEV distribution (200 m span).

Congestion type	20% trucks				50% trucks			
	μ	σ	ξ	z^*	μ	σ	ξ	z^*
SGW	2441	279.8	−0.139	3708	3399	221.7	−0.154	4358
OCT	2635	240.5	−0.105	3842	3550	177.5	−0.093	4474
HCT/OCT	2923	230.9	−0.137	3973	3973	160.8	−0.166	4644
HCT (1)	3346	257.4	−0.104	4641	4498	164.7	−0.135	5251
HCT (2)	3544	272.4	−0.110	4889	4767	210.0	−0.245	5475
FS	2490	608.0	−0.277	4379	4301	606.0	−0.294	6108

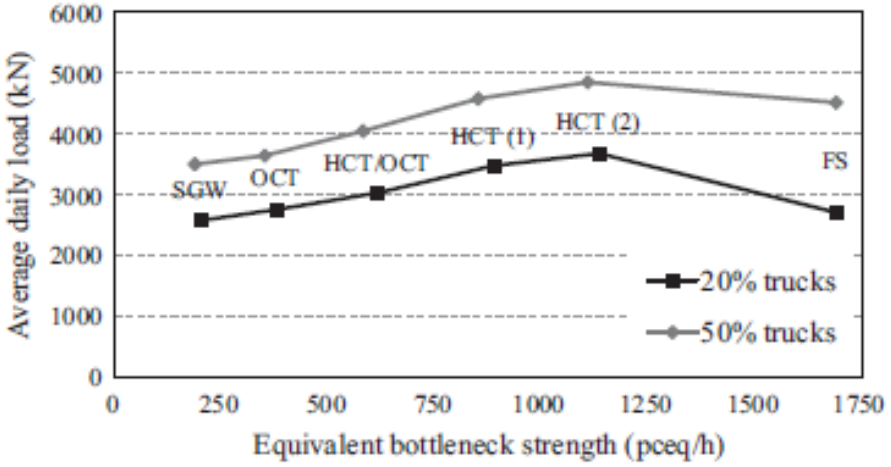

Fig. 7. Average maximum daily load on the 200-m span.

5.3 Results for 1000 m bridge

Results of simulations for the 1000 m span are given in Figure 8 and Table 6. For this longer span, the full-stop condition governs regardless of the percentage of trucks. Moreover, the separation between different congested states becomes clearer, with the congested states spread over a wider range, as local concentrations of vehicles are averaged out over the bridge length. For 50% trucks, the full-stop condition is the most critical condition for any return period. Again, the high truck percentage shows a smaller scale parameter σ (Table 6), indicating less scattering. Finally, FS conditions have again a greater scale parameter σ and a smaller shape parameter ξ.

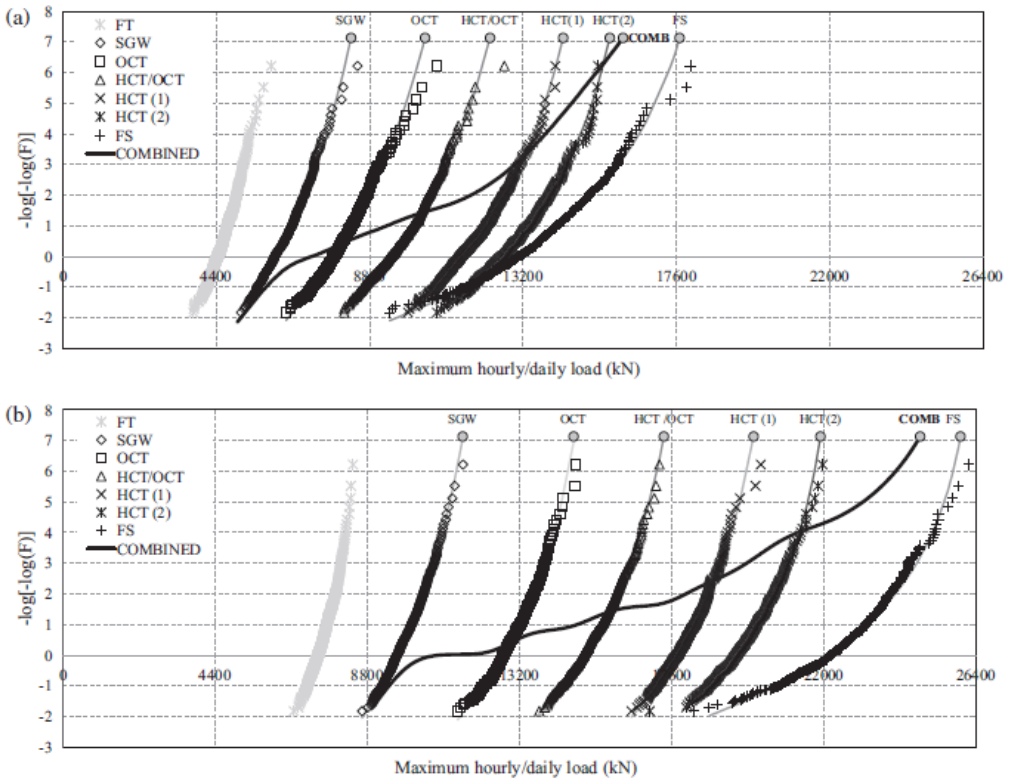

Fig. 8. Probability paper plot of total load on 1000 m span with (a) 20% and (b) 50% trucks; each vertical gridline approximately represents the weight of ten average trucks.

Table 6
Parameters and extrapolated values of the GEV distribution (1000 m span).

Congestion type	20% trucks				50% trucks			
	μ	σ	ξ	z^*	μ	σ	ξ	z^*
SGW	6092	472.0	−0.134	8262	9670	426.6	−0.147	11554
OCT	7756	567.7	−0.131	10384	12747	516.0	−0.190	14763
HCT/OCT	9385	675.8	−0.161	12251	15046	569.0	−0.174	17373
HCT (1)	11448	717.0	−0.177	14349	17755	544.0	−0.175	19970
HCT (2)	12604	825.0	−0.206	15688	19459	706.0	−0.235	21902
FS	13029	1352.0	−0.236	17691	22125	1283.0	−0.294	25954

5.4 Discussion

It should be noted that smaller inflows need stronger bottlenecks to generate congestion, so that the probability of congestion is lower. However, in the event that congestion has formed, the traffic would go straight from FT to the heavy HCT/OCT and HCT states, skipping the oscillatory congestion states SGW and OCT [50, 64]. Therefore smaller inflows do not allow the formation of oscillatory congested traffic, which returns smaller loading for the bridge, but may potentially generate critical loading events of the same order as that under a greater inflow.

Finally, a significant contribution from this work is that it should not be assumed that the full-stop condition is the most conservative design case. As shown in Section 5.2, the slow-moving HCT states can be more adverse for bridge loading than FS conditions. Note also that the full-stop condition does not depend on the inflow, unlike the other congestion states which are determined by a combination of inflow (demand) and outflow (capacity).

6. Consideration of congestion frequency

6.1 Data on congestion

Real world observations have shown that many types of congestion can occur. However, most research on bridge traffic loading assumes only queues at minimum bumper-to-bumper distances, as discussed in Section 1. Intuitively, light forms of congestion are more frequent than strong ones. Schönhof and Helbing [64] categorise more than 240 traffic breakdowns occurred on the busy A5 motorway in Germany. The most frequent extended congestion states were SGW and OCT, whereas HCT states were typical of congestion resulting from serious accidents. In that study, the FS condition was not observed. The full-stop condition is generally caused by an exceptional incident, where all the lanes need to be closed.

Data about *accident* frequency is relatively abundant in the literature. However, for bridge loading applications, it is important to know the consequences for the traffic and the road layout, rather than the cause or the severity of possible consequent injuries. On the other hand, available data about *incident* frequency and lane closure is modest. For the single-lane application considered here, it is assumed that any incident blocking at least two lanes will generate a full-stop condition, since in most highways there is a shoulder where traffic would be diverted if the driving lane were obstructed. Where an explicit incident rate is not available, Equation (8) is used to compute the *full-stop rate FSr*:

$$FSr = FS\% \times Ir = FS\% \times \frac{N \times 10^6}{ADT \times L \times T} \tag{8}$$

where *FS%* is the percentage of incidents blocking two or more lanes, *Ir* is the incident rate (the number of incidents per million vehicle kilometres travelled, I/MVkmT), *N* is the total number of incidents, *ADT* is the average daily traffic (veh/day), *L* is the length of road observed (km), and *T* is the duration of observation (days).

Tasnim et al. [76] analyse 17,796 incidents in Portland, US, in 2005. By means of Equation (8), it is possible to calculate an incident rate of about 5 I/MVkmT, with 5% of these blocking two or more lanes; it is then straightforward to deduce a full-stop rate, *FSr*, of 0.25 FS/MVkmT. Giuliano [77] suggests a rate of about 6 I/MVkmT from a smaller database of 652 incidents, with only 2% of those reported as blocking two or more lanes. Skabardonis et al. [78] report greater rates, but the site was known to be especially prone to incidents. Skabardonis et al. [79] report similar rates. Rodgers et al. [80] report a lower rate of 2.32 I/MVkmT on the M25 motorway in the United Kingdom over four weeks, with 7.6% blocking two or more lanes. These results are summarised in Table 7.

Table 7
Incident rates and full-stop rates from the literature.

Authors	Incident rate (I/MVkmT)	Incidents blocking $\geqslant 2$ lanes (%)	Full stop rate (FS/MVkmT)
Tasnim et al. [76]	≈5	5	0.25
Giuliano [77]	≈6	2	0.12
Skabardonis et al. [78]	64.6	0.6	0.39
Skabardonis et al. [79]	57.7	0.45	0.26
Rodgers et al. [80]	2.32	7.6	0.18

The Highway Capacity Manual [81] suggests that the peak hour typically carries around 10% of the average daily traffic. From the previous assumption of a peak hour flow of 1590 veh/h for the more common case of 20% trucks, an ADT of about 16 000 veh/day is derived.

Obviously, only congestion forming downstream of the bridge will affect the bridge itself. It is assumed here that incidents occurring up to 5 km downstream of the bridge will affect it. Therefore, there are 80 000 km travelled each day on the 5 km stretch, equivalent to 20 MVkmT per 250-day year. Then, using the most highly sampled rate deduced from Tasnim et al. [76], 5 full-stop events are to be expected each year. Following the previous assumption of 250 congested events per year, the full-stop frequency is found to be 2%. These values need to be adjusted for particular site-specific traffic conditions. In order to test the sensitivity of the results to these assumptions, a double full-stop frequency is considered as well.

The full-stop frequency is used to assign a distribution of congestion frequencies for the selected bottleneck strengths (Figure 9). The relative frequencies f_j sum up to 1. The curve is taken to be exponential, and is consistent with the proportions shown by Schönhof and Helbing [64].

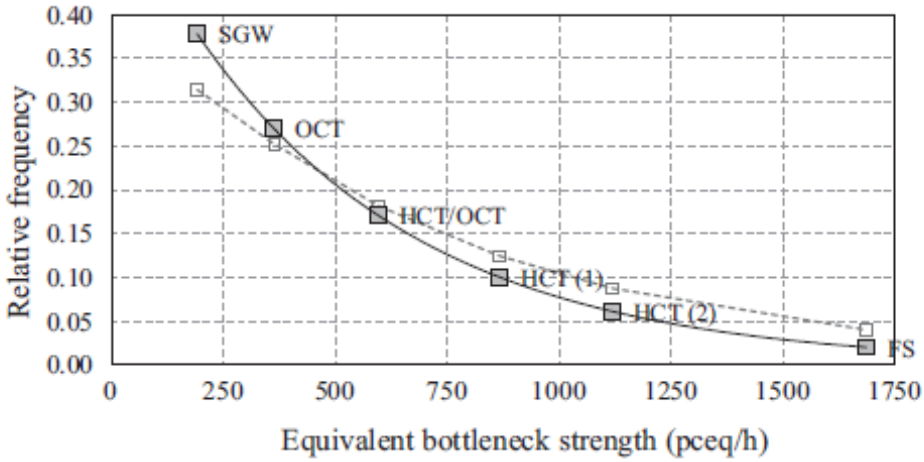

Fig. 9. Frequency of occurrence of congestion for 2% (solid) and 4% (dashed) full stop frequencies.

6.2 Combination of different congestion events

Once the congestion frequencies are assigned, it is necessary to statistically combine the six different congestion types, all of which can occur with the assigned probabilities of Figure 9. This is done by applying the law of total probability. The probability *P* that the maximum load does not exceed *z* is:

$$P(z) = \sum_{j=1}^{6} F_j(z) \cdot f_j \qquad (9)$$

in which F_j is the cumulative distribution function for the maximum load for the j^{th} congestion type (Equation (6); see also Tables 5 and 6) and f_j is the assigned probability of occurrence for that congestion type according to Figure 9. Equating *P(z)* to the target probability of 0.9992 (Section 5.1) gives the characteristic combined load, *z**.

The combined distribution function *P*(*z*) curves are shown in the probability paper plots of Figs. 6 and 8. It can be seen that the 5-year characteristic values are in the range of the strongest congestion HCT and FS, although they are less frequent. In fact, the load *z** corresponding to the target probability *P*(*z**) = 0.9992 is impossible to attain in the lightest congestions, however frequent they are, as their tails are bounded at lower values of load. On the other hand, at lower return periods, the combined load is closer to the light congestions.

Figure 10 shows the characteristic values per unit of length (EUDL, Equivalent Uniformly Distributed Load) when considering that all the congested events are of the most severe congested states (HCT(2) and FS), and combined as described above. For the 200 m span (Figure 10(a)) and 20% truck percentage, the characteristic load for the FS condition is close to the combined value (-3.3%). However, in this case it is the HCT state that is the most critical (see Figure 6(a)), thus giving a load higher by 7.9% than the combined value. As the truck percentage increases, the relative error in considering only the most severe congested state (FS) increases to 9.9%. For the 1000 m span (Figure 10(b)) and 20% trucks, the relative error due to the consideration of only one single

congestion type is 10.1%, whereas with the 50% truck percentage it drops to 4.7%. Figure 10 also confirms previous findings that EUDL decreases as the span length increases [2]. The reduction is more pronounced for lower truck percentages. On the other hand, the increase in truck percentage has a sharper effect on the load for the longer span: +23% for the 200 m span and +56% for the 1000 m span.

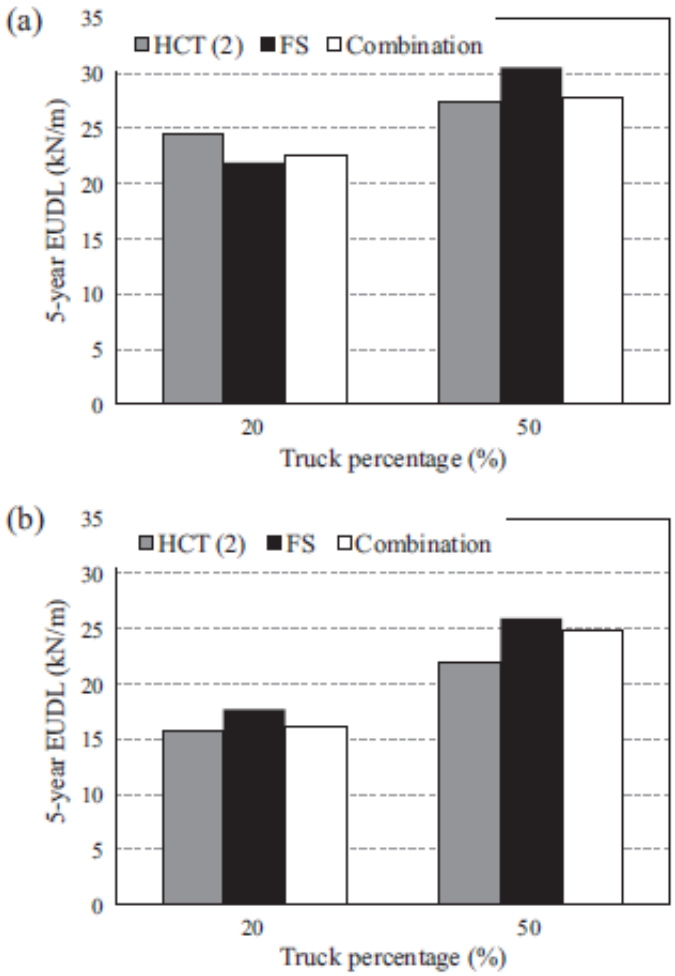

Fig. 10. Comparison of characteristic EUDL for (a) 200 m and (b) 1000 m span.

The application of the congestion frequencies based on the 4% (doubled) full-stop frequency (Figure 9) increases the characteristic combined load by between 1.1% (200 m, 20% trucks) and 2.7% (200 m, 50% trucks), suggesting that the total load is not highly sensitive to the distribution of congestion frequencies.

7. Conclusions

This paper investigates the effects of different observed congestion patterns on the total load of two long-span bridges (200 and 1000 m long). Most previous research neglects the existence of different congestion patterns, assuming only queues of vehicles at minimum bumper-to-bumper distances. Traffic micro-simulation is used here since it is a suitable tool to reproduce observed congestion patterns. Two truck percentages (20 and 50%) are considered for the simulations.

Results show that the bumper-to-bumper queue is not always the most critical loading event for the 200 m span. In fact, with 20% trucks slow-moving traffic states result in greater load than full-stop conditions. This is due to the fact that full-stop queues consider only one realisation of vehicles on the bridge, which reduces the probability of finding an extreme scenario. It is also found that oscillatory congested traffic (like *stop-and-go waves*) is not as critical for bridge loading.

A number of different congestion types will affect the bridge during its lifetime, rather than a single congestion pattern. This is taken into account by assigning a frequency of occurrence to each congestion type, based on recent data available in the literature. For the 200 m span, it is found that consideration of the sole full-stop condition slightly under-estimates the characteristic total load in the case of 20% trucks, whereas it leads to an over-estimation of the characteristic total load by about 10% when the truck percentage is 50% (representative of slow lanes in multi-lane highways). A similar over-estimation is found for the case of 1000 m span and 20% trucks; however, when considering 50% trucks, the error drops to nearly 5%. Avoiding such over-estimations may lead to significant savings in costly bridge maintenance operations.

Acknowledgements

This work is part of the TEAM project (Training in European Asset Management). The TEAM project is a Marie Curie Initial Training Network and is funded by the European Commission 7th Framework Programme (PITN-GA-2009-238648).

References

[1] Ivy RJ, Lin TY, Mitchell S, Raab NC, Richey VJ, Scheffey CF. Live loading for long-span highway bridges. American Society of Civil Engineers Transactions. 1954;119:981-1004.
[2] Buckland PG, Navin FPD, Zidek JV, McBryde JP. Proposed Vehicle Loading of Long-Span Bridges. Journal of the Structural Division. 1980;106:915-32.
[3] Ricketts NJ, Page J. Traffic data for highway bridge loading. Crowthorne: Transport Research Laboratory; 1997.
[4] Bruls A, Croce P, Sanpaolesi L, Sedlacek G. ENV 1991 - Part 3 : Traffic load on bridges - Calibration of road load models for road bridges. IABSE Colloquium. Delft1996. p. 439-53.
[5] O'Connor AJ, OBrien EJ. Traffic load modelling and factors influencing the accuracy of predicted extremes. Canadian Journal of Civil Engineering. 2005;32:270-8.
[6] Caprani CC. Lifetime highway bridge traffic load effect from a combination of traffic states allowing for dynamic amplification. Journal of Bridge Engineering. 2012;in print.
[7] Flint and Neill Partnership. Interim design standard: long span bridge loading Crowthorne: Transport and Road Research Laboratory; 1986.
[8] Nowak AS, Lutomirska M, Sheikh Ibrahim FI. The development of live load for long span bridges. Bridge Structures. 2010;6:73-9.
[9] Moses F. Calibration of Load Factors for LRFR Bridge Evaluation. Washington: National Cooperative Highway Research Program; 2001.
[10] Harman DJ, Davenport AG, Wong WSS. Traffic loads on medium and long span bridges. Canadian Journal of Civil Engineering. 1984;11:556-73.
[11] Vrouwenvelder ACWM, Waarts PH. Traffic Loads on Bridges. Structural Engineering International. 1993;3/93:169-77.

[12] Ditlevsen O, Madsen HO. Stochastic Vehicle-Queue-Load Model for Large Bridges. Journal of Engineering Mechanics. 1994;120:1829-47.
[13] Bailey SF, Bez R. Site specific probability distribution of extreme traffic action effects. Probabilistic Engineering Mechnanics. 1999;14:19-26.
[14] Prat M. Traffic load models for bridge design: recent developments and research. Progress in Structural Engineering and Materials. 2001;3:326-34.
[15] Klein LA, Mills MK, Gibson DRP. Traffic Detector Handbook. Third ed. MacLean, VA: Federal Higway Administration; 2006.
[16] OBrien EJ, Caprani CC. Headway modelling for traffic load assessment of short to medium span bridges. The Structural Engineer. 2005;83:33-6.
[17] Banks JH. Review of Empirical Research on Congested Freeway Flow. Transportation Research Record: Journal of the Transportation Research Board. 2002;1802:225-32.
[18] Ni D. Determining Traffic-Flow Characteristics by Definition for Application in ITS. IEEE Transactions on Intelligent Transportation System. 2007;8:181-7.
[19] Lipari A. Micro-simulation modelling of traffic loading on long-span bridges. Dublin: University College Dublin; 2013.
[20] Treiterer J, Myers JA. The hysteresis phenomenon in traffic flow. In: Buckley DJ, editor. 6th International Symposium on Transportation and Traffic Theory. Sydney: Elsevier; 1974. p. 13-38.
[21] Coifman B, Beymer D, McLauchlan P, Malik J. A real-time computer vision system for vehicle tracking and traffic surveillance. Transportation Research Part C. 1998;6:271-88.
[22] Hoogendoorn SP, van Zuylen HJ, Schreuder M, Gorte B, Vosselman G. Microscopic Traffic Data Collection by Remote Sensing. Transportation Research Record: Journal of the Transportation Research Board. 2003;1855:121-8.
[23] Federal Highway Administration. NGSIM Project. Federal Highway Administration; 2005.
[24] Blacoe S, Caprani CC, OBrien EJ, Lipari A. Determination of Minimum Gap in Congested Traffic. In: Caprani C, O'Connor A, editors. Bridge and Concrete Research in Ireland. Dublin2012. p. 31-6.
[25] OBrien EJ, Hayrapetova A, Walsh C. The use of micro-simulation for congested traffic load modelling of medium- and long-span bridges. Structure and Infrastructure Engineering. 2012;8:269-76.
[26] Zaurin R, Catbas FN. Integration of computer imaging and sensor data for structural health monitoring of bridges. Smart Materials and Structures. 2010;19:1-15.
[27] European Committee for Standardization. Eurocode 1: Actions on Structures. Part 2: Traffic loads on bridges: CEN; 2003.
[28] Bruls A, Calgaro J-A, Mathieu H, Prat M. ENV 1991 - Part 3 : The main models of traffic loads on road bridges - Background studies. IABSE Colloquium. Delft1996. p. 215-28.
[29] O'Connor AJ, Jacob B, OBrien EJ, Prat M. Report of Current Studies Performed on Normal Load Model of EC1. Revue française de génie civil. 2001;5:411-33.
[30] British Standard. Steel, concrete and composite bridges. Part 2: Specification for loads. London: British Standards Institution; 2006.
[31] Consiglio Superiore dei Lavori Pubblici. Norme Tecniche per le Costruzioni. Capitolo 5 - Ponti: Consiglio Superiore dei Lavori Pubblici; 2008.
[32] The Highways Agency. Design Manual for Roads and Bridges. Volume 3, Section 4, Part 2: Technical Requirements for the Assessment and Strengthening Programme for Highway Structures (Stage 3 - Long span bridges). London: The Stationery Office; 1992.

[33] The Highways Agency. Design Manual for Roads and Bridges. Volume 3, Section 4, Part 19: The Assessment of Highway Bridges and Structures for the Effects of Special Types General Order (STGO) and Special Order (SO) Vehicles. London: The Stationery Office; 2011.
[34] American Association of State Highway and Transportation Officials. AASHTO LRFD Bridge Design Specifications - Fifth edition. Washington: American Association of State Highway and Transportation Officials; 2010.
[35] Buckland PG. North American and British Long-Span Bridge Loads. Journal of Structural Engineering. 1991;117:2972-87.
[36] American Association of State Highway and Transportation Officials. Standard Specifications for Highway Bridges, 17th Edition. Washington: American Association of State Highway and Transportation Officials; 2002.
[37] Nowak AS. Calibration of LRFD Bridge Code. Journal of Structural Engineering. 1995;121:1245-51.
[38] Lutomirska M. Live Load Models for Long Span Bridges. Lincoln: University of Nebraska; 2009.
[39] Committee on Loads and Forces on Bridges of the Committee on Bridges of the Structural Division. Recommended design loads for bridges. Journal of the Structural Division. 1981;107:1161-213.
[40] American Association of State Highway and Transportation Officials. The Manual for Bridge Evaluation - Second Edition. Washington: American Association of State Highway and Transportation Officials; 2011.
[41] Chen SR, Wu J. Modeling stochastic live load for long-span bridge based on microscopic traffic flow simulation. Computers and Structures. 2011;89:813-24.
[42] Nagel K, Schreckenberg M. A cellular automaton model for freeway traffic. Journal de Physique I France. 1992;2:2221-9.
[43] Caprani CC. Calibration of a Congestion Load Model for Highway Bridges Using Traffic Microsimulation. Strucural Engineering International. 2012;22:342-8.
[44] Enright B, Carey C, Caprani CC. Microsimulation Evaluation of Eurocode Load Model for American Long-Span Bridges. Journal of Bridge Engineering. 2013;18:1252-60.
[45] Brackstone M, McDonald M. Car following: a historical review. Transportation Research Part F. 1999;2:181-96.
[46] Hoogendoorn SP, Bovy PHL. State-of-the-art of vehicular traffic modelling. Proceedings of the Institution of Mechanical Engineers, Part I: Journal of Systems and Control Engineering. 2001;215:283-303.
[47] Orosz G, Wilson RE, Stépán G. Traffic jams: dynamics and control. Philosophical Transactions of the Royal Society A. 2010;368:4455-79.
[48] Dowling R, Skabardonis A, Alexiadis V. Traffic Analysis Toolbox Volume III: Guidelines for Applying Traffic Microsimulation Software. Washington: Federal Highway Administration; 2004.
[49] Hidas P, Wagner P. Review of Data Collection Methods for Microscopic Traffic Simulation. Proceedings of the World Conference on Transport Research. Istanbul2004.
[50] Treiber M, Hennecke A, Helbing D. Congested Traffic States in Empirical Observations and Microscopic Simulations. Physical Review E. 2000;62:1805-24.
[51] Sparmann U. The importance of lane-changing on motorways. Traffic Engineering & Control. 1979;20:320-3.

[52] Fwa TF, Li S. Estimation of Lane Distribution of Truck Traffic for Pavement Design. Journal of Transportation Engineering. 1995;121:241-8.
[53] Treiber M, Kesting A. Validation of traffic flow models with respect to the spatiotemporal evolution of congested traffic patterns. Transportation Research Part C. 2012;21:31-41.
[54] Kesting A, Treiber M. Calibrating Car-Following Models by Using Trajectory Data. Transportation Research Record: Journal of the Transportation Research Board. 2008;2088:148-56.
[55] Chen C, Li L, Hu J, Geng C. Calibration of MITSIM and IDM Car-Following Model Based on NGSIM Trajectory Datasets. International Conference on Vehicular Electronics and Safety. QingDao (China)2010. p. 48-53.
[56] Hoogendoorn SP, Hoogendoorn R. Calibration of microscopic traffic-flow models using multiple data sources. Philosophical Transactions of the Royal Society A. 2010;368:4497-517.
[57] Brockfeld E, Kühne RD, Wagner P. Calibration and validation of microscopic traffic flow models. Transportation Research Record: Journal of the Transportation Research Board. 2004;1876:62-70.
[58] Punzo V, Simonelli F. Analysis and Comparison of Microscopic Traffic Flow Models with Real Traffic Microscopic Data. Transportation Research Record: Journal of the Transportation Research Board. 2005;1934:53-63.
[59] Treiber M, Kesting A. Traffic Flow Dynamics: Data, Models and Simulation: Springer; 2013.
[60] Kesting A, Treiber M. How reaction time, update time, and adaptation time influence the stability of traffic flow. Computer-Aided Civil and Infrastructure Engineering. 2008;23:125-37.
[61] Kerner BS, Rehborn H. Experimental features and characteristic of traffic jams. Physical Review E. 1996;53:R1297-R300.
[62] Cassidy MJ, Bertini RL. Some traffic features at freeway bottlenecks. Transportation Research Part B. 1999;33:25-42.
[63] Transportation Research Board. Highway Capacity Manual HCM 2010. Volume 2: Uninterrupted flow. Washington: Transportation Reseach Board; 2010.
[64] Schönhof M, Helbing D. Empirical Features of Congested Traffic States and Their Implications for Traffic Modelling. Transportation Science. 2007;41:135-66.
[65] Zielke BA, Bertini RL, Treiber M. Empirical Measurement of Freeway Oscillation Characteristics: An International Comparison. Transportation Research Record: Journal of the Transportation Research Board. 2008;2088:57-67.
[66] Caprani CC, Enright B, Carey C. Lane changing control to reduce traffic load effect on long-span bridges. In: Biondini F, Frangopol DM, editors. 6th International Conference on Bridge Maintenance, Safety and Management. Stresa: Taylor and Francis; 2012.
[67] Hallenbeck M, Rice M, Smith B, Cornell-Martinez C, Wilkinson J. Vehicle volume distribution by classification. Federal Highway Administration; 1997.
[68] Knospe W, Santen L, Schadschneider A, Schreckenberg M. Single-vehicle data of highway traffic: microscopic description of traffic phases. Physical Review E. 2002;65.
[69] The Council of the European Union. Official Journal of the European Communities. Council Directive 96/53/EC of 25 July 1996 laying down for certain road vehicles circulating within the Community the maximum authorized dimensions in national and international traffic and the maximum authorized weights in international traffic1996. p. L235/59-75.
[70] Grave SAJ, OBrien EJ, O'Connor AJ. The determination of site-specific imposed traffic loadings on existing bridges. In: Ryall MJ, Parke GAR, Harding JE, editors. Bridge Management 4: Thomas Telford; 2000. p. 442-9.

[71] Wardrop JG. Some Theoretical Aspects of Road Traffic Research. Proceedings of the Institution of Civil Engineers: Engineering Divisions. 1952;1:325-62.
[72] Hall FL. Traffic Stream Characteristics. In: Gartner N, Messer CJ, Rathi AK, editors. Revised Monograph on Traffic Flow Theory: Federal Highway Administration; 1994.
[73] Lipari A, OBrien EJ, Caprani CC. A comparative study of a bridge traffic load effect using micro-simulation and Eurocode load models. In: Biondini F, Frangopol DM, editors. 6th International Conference on Bridge Maintenance, Safety and Management. Stresa: Taylor and Francis; 2012.
[74] Coles S. An Introduction to Statistics Modeling of Extreme Values. London: Springer; 2001.
[75] Ang AH-S, Tang WH. Probability Concepts in Engineering: Emphasis on Application to Civil and Environmental Engineering, 2nd Edition. Hoboken: Wiley; 2007.
[76] Tasnim S, Monsere CM, Bertini RL. Toward an Automated Incident Analysis Process Using Archived Data on the Portland Oregon Freeway System. 10th International Conference on Application of Advanced Technologies in Transportation. Athens2008.
[77] Giuliano G. Incident characteristics, frequency, and duration on a high volume urban freeway. Transportation Research Part A. 1989;23:387-96.
[78] Skabardonis A, Petty KF, Bertini RL, Varaiya PP, Noeimi H, Rydzewski D. I-880 Field Experiment: Analysis of Incident Data. Transportation Research Record. 1997;1603:72-9.
[79] Skabardonis A, Petty KF, Varaiya PP. Los Angeles I-10 Field Experiment: Incident Patterns. Transportation Research Record. 1999;1683:22-30.
[80] Rodgers S, Wadsworth B, Smith SD, Forde MC. An analysis of road traffic incidents on the M25 motorway, UK. Proceedings of the ICE - Transport. 2006;159:1-8.
[81] Transportation Research Board. Highway Capacity Manual - Fourth Edition. Transportation Research Board; 2000.